



AUSTRALIAN ATOMIC ENERGY COMMISSION
RESEARCH ESTABLISHMENT

LUCAS HEIGHTS RESEARCH LABORATORIES

NEUTRONIC MODELS FOR THE HIFAR REACTOR

by

B.V. HARRINGTON

September 1983

ISBN 0 642 59781 2

AUSTRALIAN ATOMIC ENERGY COMMISSION
RESEARCH ESTABLISHMENT
LUCAS HEIGHTS RESEARCH LABORATORIES

NEUTRONIC MODELS FOR THE HIFAR REACTOR

by

B.V. HARRINGTON

ABSTRACT

Standard neutronic models have been developed for the AAEC's materials testing reactor HIFAR, and are available as members of a partitioned data set. The models have been used to calculate reactor physics parameters related to operation and safety. Results from the calculations are presented.

National Library of Australia card number and ISBN 0 642 59781 2

The following descriptors have been selected from the INIS Thesaurus to describe the subject content of this report for information retrieval purposes. For further details please refer to IAEA-INIS-12 (INIS: Manual for Indexing) and IAEA-INIS-13 (INIS: Thesaurus) published in Vienna by the International Atomic Energy Agency.

BURNUP; COMPUTER CALCULATIONS; HIFAR REACTOR; NEUTRON FLUX; REACTIVITY;
REACTIVITY WORTHS; TEMPERATURE COEFFICIENT; VOID COEFFICIENT

CONTENTS

1. INTRODUCTION	1
2. A TYPICAL LOW RIG BURDEN HIFAR OPERATING PROGRAM	2
3. FUEL DESCRIPTION AND DATA	2
4. D ₂ O REFLECTOR FACILITIES AND SAFETY RODS	4
5. THE HIFAR MODELS	4
5.1 AUS Modules	5
5.2 The BVHIFXS Model	5
5.3 The BVHIFCEL Model	6
5.4 The BVHIFRZ Model	6
5.5 The BVHFXYA2 and BVHFXYE2 Models	7
6. RESULTS	9
6.1 The Fine Flux Factor	9
6.2 Flux Depression Caused in the Fuel by a Rig	9
6.3 Variation of Flux with Burnup	10
6.4 Core Position Factors	10
6.5 Reactivity Loss with Fuel Burnup	11
6.6 Variation of Epithermal to Thermal Flux Across the Core	11
6.7 Absorber Coefficients	12
6.8 Reactivity Coefficients and Other Safety Related Parameters	12
7. CONCLUSIONS	13
8. REFERENCES	13

(Continued)

Table 1	Data for HIFAR operating programs 243-252	15
Table 2	Reactivity controlled by rigs and facilities in the average fuel models	15
Table 3	Reactivity controlled by rigs during OP251	16
Table 4	Variation of cell flux shape with burnup	17
Table 5	Flux depression in fuel caused by a rig	18
Table 6	Flux variation with burnup	18
Figure 1	End-of-program 251 fuel loading	19
Figure 2	BVHIFXS fuel cell geometry	20
Figure 3	BVHIFRZ geometry	21
Figure 4	Core position factors	22
Figure 5	Absorber coefficients	22
Figure 6	Reactivity variation with fuel mass	23
Figure 7	Fuel plus poison coefficients	24
Figure 8	Cell-average, mid-plane epithermal/thermal flux ratios	24
Figure 9	Fuel plus coolant temperature coefficients	25
Figure 10	Coolant void coefficients	25
Appendix A	BVHIFXS, BVHIFCEL, BVHIFRZ and BVHFXA2 listings	27

1. INTRODUCTION

Because of the recurring need for reactor physics calculations for the AAEC's materials testing reactor HIFAR, a standard set of calculational models has been developed. These models provide a set of procedures for calculating reactor physics parameters and are input to codes in the form of card image data sets on disk. The AUS modular scheme for reactor calculations [Robinson 1975a] has been used. Earlier HIFAR models produced an almost flat flux across the core, and very high excess reactivities, hence could not be used with any degree of confidence. There was no single explanation for the inadequacies of these models, but to overcome them it was necessary to include, in some detail, all the D₂O reflector facilities. The models are based on HIFAR Operating Program 251 (OP 251) which was typical of the low rig burden operating programs in 1978-1979.

The following standard models have been developed and are available on the UNED [Cawley 1983] data set BVH.HIFAR:

- (a) BVHIFXS - a five-group smeared cross section preparation model. Fuel cross sections are produced as a function of burnup for use in the models BVHIFRZ, BVHFXYA2 and BVHFXYE2.
- (b) BVHIFRZ - a cylindrical diffusion model. Energy-dependent axial bucklings for each region are produced for use in the HIFAR XY geometry diffusion models BVHFXYA2 and BVHFXYE2.
- (c) BVHFXYA2 - a two-dimensional XY geometry diffusion model with average end of OP 251 burnup throughout the core.
- (d) BVHFXYE2 - a two-dimensional XY geometry diffusion model with the explicit end of OP 251 fuel loadings for each fuel element.
- (e) BVHIFCEL - an 'average' fuel cell calculation. The composition of the fuel is the average at the end of OP 251 and includes fission products.

Although these models were developed for a specific HIFAR operating program, they should be useful, with little or no change, for any operating program. The models have been used to calculate reactor physics parameters related to operation and safety. The results are discussed in Section 6.

2. A TYPICAL LOW RIG BURDEN HIFAR OPERATING PROGRAM

Core weights, reactivities and rig burdens for OP 251 and the comparable ranges for OPs 243-252 are summarised in Table 1. A detailed account of the reactivities controlled by the in-core and heavy water facility rigs is given in Table 2. Modified values for reflector rig burdens were received in May 1982 and have been incorporated in models BVHFXYA2 and BVHFXYE2; in all other respects, these resemble the earlier models BVHFXYA1 and BVHFXYE1. Although air-cooled in-core rigs were present in some of the programs considered, the in-core rigs in OP 251 were in perforated aluminium liners.

The end of OP 251 fuel loadings used in the models are given in Figure 1 together with the convention for labelling fuel element positions. The end of program has been used since the reactivity controlled by the coarse control arms (CCAs) at that time is minimal. The CCAs have been omitted from the calculational models.

Note that the percentage reactivity ($\rho\%$) used is $((k_{\text{eff}}-1)/k_{\text{eff}}) \times 100$. All reactivities quoted in this report are relative to a 3.2 kg core. To convert the reactivity $\rho'\%$ in a core of mass M to a reactivity $\rho\%$ in a 3.2 kg core, the following conversion has been used [Harries 1978]:

$$\rho = \rho' \left(\frac{M}{3.2} \right)^{0.7}$$

3. FUEL DESCRIPTION AND DATA

In OP 251, as in all programs after OP 247, only 150 g Mark 4/5 fuel elements were used. The Mark 4/5 fuel element consists of four concentric fuel tubes, an outer aluminium casing and an inner aluminium liner. Each fuel tube consists of three curved U/A1 alloy fuel plates completely encased in aluminium cladding and joined by electron beam welding. Because of the aluminium seams between the plates, the fuel 'meat' occupies an average of 90.89 vol.% of the core annulus (taken over the active core height). The dimensions of this element are listed below and have been derived from reference drawings supplied by British Nuclear Fuels Ltd, the United Kingdom Atomic Energy Authority and the AAEC. Fuel tubes are numbered from the inner-most. The plates are numbered to correspond with the tubes in which they are used.

Overall Fuel Plate Dimensions

Length 66 cm Thickness 0.1524 cm

Width before curving:

	(cm)
plate 1	6.574
plate 2	7.600
plate 3	8.626
plate 4	9.652

Core Dimensions

Length 60.325 cm Thickness 0.06604 cm

Nominal width before curving:

	(cm)
plate 1	5.786
plate 2	6.812
plate 3	7.838
plate 4	8.865

Inside Diameter of Tubes

	(cm)
Fuel tube 1	6.078
Fuel tube 2	7.058
Fuel tube 3	8.039
Fuel tube 4	9.020

Core Composition

Total uranium in U/Al alloy 17 wt.% ^{235}U enrichment 80%

^{235}U content per plate:

	(g)
plate 1	9.9
plate 2	11.6
plate 3	13.4
plate 4	15.1

Inner Aluminium Liner

Inside diameter 5.0724 cm Outside diameter 5.3975 cm

Outer Aluminium Casing

Inside diameter 9.983 cm Outside diameter 10.300 cm

4. D₂O REFLECTOR FACILITIES AND SAFETY RODS

The following information is represented in the XY diffusion models, but the small 2TAN facility has been omitted. The horizontal experimental facilities projecting into the heavy water consist of eight re-entrant aluminium thimbles welded to the reactor aluminium tank (RAT). Each re-entrant tube contains either an aluminium or stainless steel liner. The 10H, 6H and 4H horizontal facilities are, respectively, 10 in (25.4 cm), 6 in (15.24 cm) and 4 in (10.16 cm) in diameter. The 10H and 6H facilities are at the mid-plane of the reactor, whereas the six 4H holes are distributed at the top and bottom of the core in symmetric pairs. The vertical reflector facilities consist of flooded aluminium tubes, of which four are 6 in (15.24 cm) diameter tubes (6V), five are 4 in (10.16 cm) tubes (4V) and nine are 2 in (5.08 cm) tubes (2V).

Since both safety rods are held fully out during normal operation, the interiors of the static sleeves are assumed to be void. The outer and inner diameters of the aluminium safety rod sleeves are 5.4 and 4.45 cm respectively. Details of the horizontal and vertical facilities and the safety rod sleeves were obtained from H. Moeskops [AAEC private communication].

5. THE HIFAR MODELS

The HIFAR models BVHIFXS, BVHIFCEL, BVHIFRZ and BVHFXYA2 are listed in Appendix A.

5.1 AUS Modules

The following modules from the reactor code scheme AUS [Robinson 1975a] were used:

- MIRANDA a cross section data preparation module which uses multiregion resonance theory and a 128-group cross section library derived from ENDFB/IV data [Robinson 1977].
- ANAUSN a one-dimensional multigroup S_N transport module [Clancy 1982].
- CHAR a burnup module [Robinson 1975b].
- POW a two-dimensional multigroup neutron diffusion module [Pollard 1974].
- EDIT calculates reaction rates and produces a group collapsed and smeared material cross section library [J.P. Pollard, AAEC unpublished document].
- MERGEL merges two AUS cross section libraries.

5.2 The BVHIFXS Model

The fuel cell geometry and layout used in the BVHIFXS calculations are given in Figure 2. The cell is based on a fuel lattice pitch of 6 in (15.24 cm) and has a reflective boundary condition.

A D_2O purity of 99.27 wt % and an operating temperature of 323 K are assumed [J. Bezimienny, AAEC private communication]. At 50°C, the heavy and light water densities are taken to be 1.0957 g cm⁻³ and 0.988 g cm⁻³ respectively. Boundaries separating the five energy groups are 0.82 MeV, 9.12 keV, 1.13 eV and 0.14 eV.

The AUS modules listed in Section 5.1 are used in a loop to generate smeared five-group core cross sections as a function of burnup. MIRANDA produces 25-group cross sections using multiregion resonance theory. These cross sections are used in an ANAUSN radial fuel cell calculation. ANAUSN is followed by EDIT to produce smeared 5-group fuel cell cross sections as well as cross sections for a 1/v absorber (i.e. one for which the absorption cross

section is inversely proportional to neutron velocity). CHAR is used to do a nuclide burnup calculation at the constant thermal flux of 1.17×10^{14} , which gives an average power of 10/25 MW per element over a core residence time of approximately 173 days. This is equivalent to a discharge content of approximately 64 g ^{235}U per element. Time steps are chosen for CHAR to give approximately equal burnup per time step. The calculational sequence is then repeated from MIRANDA, using the burnt fuel composition.

Five-group reflector data (i.e. data for D_2O , graphite, aluminium and stainless steel) are produced directly from the 128-group ENDFB/IV library data [Garber 1975] by the AUS module MIRANDA.

5.3 The BVHIFCEL Model

The average fuel cell (93.5 g ^{235}U) model uses interpolated fuel and fission product concentrations derived from the burnup-dependent results of BVHIFXS. Calculations involve the use of the AUS modules MIRANDA, ANAUSN, and EDIT. BVHIFCEL is used to generate smeared fuel cell cross sections for use in the XY model perturbation calculations.

5.4 The BVHIFRZ Model

This model provides a POW diffusion calculation of HIFAR in RZ geometry using interpolated cross section data produced by BVHIFXS. The layout and geometry are shown in Figure 3. An average end of OP 251 core composition of 93.5 g ^{235}U per element is assumed. No attempt is made to represent the in-core rigs. In the XY model BVHFXA1, the detailed representation of the reflector facilities and safety rod thimbles accounts for 4.95 per cent reactivity. In the RZ model, the vertical facilities and the safety rod thimbles and voids controlling 1.45 per cent reactivity are represented as aluminium smeared out in regions 6 and 7, whereas the D_2O rigs and horizontal facilities controlling 3.5 per cent reactivity are represented by aluminium over the core height only, i.e. region 6. A concentration search routine was used to determine the aluminium volume fractions. The aluminium in the fuel element extensions is included as aluminium in region 2. An estimated 2.2 vol.% aluminium has been included in region 3 of the axial reflector. The reactivity controlled by the aluminium in the axial reflector above the core is 0.24 per cent in region 2, and 0.57 per cent in region 3. The material volume fractions in each region of Figure 3 are as follows:

Region 1	fuel			
Region 2	D ₂ O	0.902	A1	0.098
Region 3	D ₂ O	0.978	A1	0.022
Region 4	A1			
Region 5	graphite			
Region 6	D ₂ O	0.91239	A1	0.03761
Region 7	D ₂ O	0.98466	A1	0.01535

The calculated end-of-program reactivity for this model is 2.82 per cent.

Mid-plane region and energy-dependent axial bucklings are produced for use in the XY models BVHFXA1, BVHFXA2, BVHFXE1 and BVHFXE2. The preference for the mid-plane bucklings is due to the greater accuracy of perturbation calculations in mid-plane XY models than in the axial average models. Because mid-plane bucklings are used, the calculated fluxes are strictly values for the core mid-plane. However, as the axial form factor for the thermal flux shows little radial variation, both power and thermal flux can be treated as either mid-plane or axial-average values if an appropriate normalisation is used. (The calculated form factor is 1.044.) The spectrum varies with axial position and the calculated values should be treated as mid-plane values.

5.5 The BVHFXA2 and BVHFXE2 Models

BVHFXA1 and BVHFXE1 are two-dimensional XY models at the end of OP 251, with average and explicit fuel element loadings respectively. Representations of the horizontal and vertical heavy water facilities, voided safety rod thimbles and rigs are included in both models. A partial breakdown of reactivities controlled by them in BVHFXA1 is given in Table 2. Each rig is represented by the amount of thermal absorber required to give the measured reactivity; all other reflector details are calculated. Except where otherwise stated, these are the two-dimensional XY models which have been used. BVHFXA2 and BVHFXE2 are identical to these models in every respect, other than the reflector rig burdens which have been modified to allow for new values received in May 1982 (Table 3).

The horizontal facilities are difficult to represent in the XY models, particularly as their reactivity worth is difficult to estimate. A two-dimensional discrete ordinate code DOT [Rhoades and Mynatt 1973] was used to estimate the effect of the 10H void on HIFAR power distribution and reactivity. For the RZ DOT calculation, HIFAR was very roughly approximated

by a cylinder with the axis of 10H as the Z axis. Calculations with and without the 10H void showed that the void caused reductions of 0.4 per cent in the reactivity and 8.5 per cent in the power fraction of the nearest fuel element [B.J. McGregor, AAEC private communication]. These results were used to 'converge', by trial and error, to a representation of 10H. In BVHFXA1, the density of D₂O is reduced by the ratio of the void volume to the 'volume' in which 10H is represented, and the resulting diffusion coefficients are doubled to allow for streaming; this produces the required change in the power fraction, and a reduction of 0.35 per cent in reactivity. The core height is used to define the volume in the XY representation. The reduced density of the D₂O and the modified diffusion coefficients are used to represent the 10H, 6H and 4H facilities in the XY models. Areas representing the 6H and 4H facilities in the XY models are chosen such that the relationship of actual void volume to volume of representation is the same as the density reduction for the D₂O.

From DOT calculations, it was observed that results were sensitive to the distance of the void from the core. Hence, within the limitations of an XY model, care was taken to position these facilities to preserve their distances from the core. The aluminium and stainless steel for the horizontal facility tubes and liners are represented in the mid-plane by weighting for volume and reactivity worth. The reactivity worths were obtained as a function of height from the RZ model BVHIFRZ.

The vertical aluminium safety rod thimble and D₂O facility thimbles are included explicitly. The voids in the safety rod liners are approximated by an equivalent amount of aluminium. The 2V7 void and aluminium reactivity burdens of 0.041 and 0.045 per cent respectively [Connolly and McKenzie 1960] were used to estimate the equivalent aluminium concentration. It was assumed that for similar void diameters,

$$\frac{\text{worth of void/area of void}}{\text{worth of aluminium/area of aluminium}} = \text{constant}$$

The in-core and D₂O rigs are represented by a thermal absorber. Perturbation calculations with the thermal absorber included successively in each of the rig positions gave a first approximation to the required concentrations. Improved values were obtained by repeating the perturbation calculation, but using a perturbed real flux and an unperturbed adjoint flux.

BVHFXYE2 differs from BVHFXYA2 only in that it uses the actual end of OP 251 fuel loading in each fuel position, rather than the average value of 93.5 g ^{235}U per fuel element.

The calculated end-of-program reactivity of 0.84, 0.04 and 1.49 per cent for the models BVHFXYA1, BVHFXYA2 and BVHFXYE1, respectively, compares satisfactorily with the observed shutdown reactivity of 1.43 per cent for OP 251.

6. RESULTS

The HIFAR models have been used to calculate reactor physics parameters related to operation and safety. Where possible, the results have been compared with those of Duerden [1973], who presented a compilation of experimentally derived parameters for HIFAR.

6.1 The Fine Flux Factor

The thermal flux on the axis of a fuel element can be measured; however, for fuel management the average thermal flux in the fuel element is needed. The ratio of the fuel average to the fuel centre line (CL) thermal flux (known as the fine flux factor) is summarised in Table 4 as a function of burnup. These fine flux factors were calculated using BVHIFXS and are 2 per cent lower than those calculated by D. Culley [cited in Duerden 1973]. The ratio of fuel to cell average thermal flux is also summarised for use with core position factors (Figure 4) and the cell average absorber coefficients (Figure 5).

6.2 Flux Depression Caused in the Fuel by a Rig

Modified versions of BVHIFCEL were used to produce cross sections for fuel cells in which rigs with MoO_3 , UO_2 and Ir samples were included. An earlier version of BVHIFRZ was used for reactor calculations in which these rigs were included in the hollow fuel element (HFE) in the central position C3. The calculated fuel thermal flux depressions are compared in Table 5 with values obtained using Culley's formula for relating flux depression to rig worth [cited in Duerden 1973]. The calculations indicate that the flux depression is probably dependent on the sample used rather than on the rig worth. It is however impractical to consider the details of the various samples loaded in each fuel element, particularly as they change during an

operating program. A modified version [G.S. Robinson, AAEC private communication] of Culley's formula estimates the MoO₃ and Ir flux depressions reasonably well:

$$C_i = 1 - 0.12008\rho' + 0.6232(\rho')^2 - 0.01224(\rho')^3$$

where C_i is the rig flux depression factor and ρ' is the equivalent reactivity worth of the rig in a 3.2 kg core and in C3 position. This depression factor was used to adjust subsequent data to remove the effect caused by the presence of rigs.

6.3 Variation of Flux with Burnup

Central element replacement calculations, using a modified version of BVHIFRZ, were undertaken with the central element replaced by fuel of varying burnup. HIFAR OP 277 was used with an end-of-program core mass of 2467 g ²³⁵U, of which 128.06 g was in the centre element and an average of 97.456 g in other elements.

Cell average fluxes were calculated as a function of burnup and converted to CL thermal fluxes using ratios from Table 4. Centre line thermal fluxes and epithermal to thermal flux ratios are summarised as a function of burnup in Table 6. The Westcott thermal flux and epithermal flux in the range 9.1 keV to 1.1 eV have been used. Contrary to the conclusions of Duerden [1973], based on routine measurements made during earlier operating programs, the CL thermal flux shape is decidedly non-linear. The epithermal to thermal flux ratio indicates a softening of the spectrum with burnup. This is not inconsistent with Duerden's claim that there is no significant change in spectrum, since the calculated spectrum shift is of the same order of magnitude as errors in the measurements discussed by Bicevskis et al. [1967].

6.4 Core Position Factors

The core position factor is the ratio of the axially averaged CL thermal flux in the HFE position to the mid-plane CL thermal flux in C3. Cell averaged thermal fluxes produced by BVHFXA2 have been used to calculate the core position factors. They have been adjusted to remove the effect of rigs (Section 6.2) and are shown in Figure 4. The explicit core loading model was used to investigate the dependence of the core position factors on the fuel management scheme. The flux variation with ²³⁵U mass (Table 6) was used to

make the two sets of core position factors directly comparable. Good agreement was obtained in the central fuel element positions, but the average fuel loading model overestimated the core position factors in the outer positions by as much as 4.5 per cent. When compared with the core position factors published by Duerden [1973], those given in Figure 4 appear to be poor near the 10H and 6H horizontal facilities, and seem to tilt from the top to the bottom of the core. Differences in some outer positions are as high as 20 per cent, whereas that for B1 is close to 40 per cent.

6.5 Reactivity Loss with Fuel Burnup

The central fuel element replacement calculations (Section 6.3) were used to calculate the reactivity worth of new fuel and burnt fuel as a function of ^{235}U mass (Figure 6). The burnt fuel includes the long-lived fission products and ^{135}Xe and ^{149}Sm . From Figure 6, it is seen that the fuel worth per g ^{235}U obtained by replacing a new 115 g ^{235}U fuel element by a new 150 g element is approximately 0.013; this is lower than the value of 0.0153 measured by Duerden [1973]. However, the approximate fuel worth of 0.015 $\rho\%$ per g ^{235}U derived from a straight line approximation over the operating range of fuel mass (approximately 70 to 150 g ^{235}U) agrees well with the central element fuel worth of 0.0153 currently in use in fuel management.

Fuel plus poison coefficients for high burnup (i.e. to 93.5 g ^{235}U) at all fuel element positions have been calculated by perturbation theory using BVHFXA2, and successively replacing each 93.5 g element with a burnt 92.5 g element. The coefficients (Figure 7) include the long-lived poisons and ^{135}Xe and ^{149}Sm . Fuel plus poison coefficients were also calculated for a low burnup core with fuel elements burnt to 107.78 g ^{235}U . The core average fuel plus poison coefficients ($\rho\%$ per g ^{235}U burnup) for low and high burnup fuel were -1.033×10^{-2} and -1.078×10^{-2} respectively. The C3 fuel plus poison coefficients for low and high burnup values were -1.604×10^{-2} and -1.658×10^{-2} respectively.

6.6 Variation of Epithermal to Thermal Flux Across the Core

Cell-averaged mid-plane epithermal to thermal flux ratios, calculated using the average core loading model BVHFXA2 and adjusted to remove the effect of rigs, are given in Figure 8. These ratios were also calculated using the explicit core model, and adjusted for the ^{235}U mass difference by using the epithermal to thermal flux dependence on burnup (Table 6). In

general, the average core loading model underestimated the ratio in the centre by up to 6 per cent and, for the outer fuel elements, overestimated it by up to 5 per cent. The difference in the overall shape of the ratio was probably due to the fuel management scheme which concentrates fuel elements with a high ^{235}U content at the centre, and those with a low ^{235}U content on the outside. The random scatter in the differences, superimposed on the difference in shape, may be due to central element replacement results in Table 6 being somewhat inaccurate for elements in other positions.

6.7 Absorber Coefficients

The reactivity worths of $1/v$ absorber in the fuel element positions (evenly distributed over 6 in x 6 in (15.24 cm x 15.24 cm) were calculated by perturbation theory using BVHFXA2 and are given in Figure 5. To investigate the dependence of absorber worth on fuel burnup, the calculation was repeated with a core consisting of fuel elements burnt to only 107.78 g ^{235}U , i.e. a core mass of 2.6945 kg ^{235}U . The calculated core average absorber coefficients for the low and high burnup cases are -1.449×10^{-4} and -1.493×10^{-4} $\rho\%$ per cm^2 , respectively.

6.8 Reactivity Coefficients and Other Safety Related Parameters

Perturbation calculations with the XY model were used to derive void and temperature (excluding expansion) reactivity coefficients. The RZ model was used to calculate the prompt neutron lifetime, the effective delayed neutron fraction and the top reflector worth. The following is a summary of the results:

Total fuel temperature coefficient ($\delta k/k$ per $^{\circ}\text{C}$)	-1.1×10^{-6}
Total fuel plus coolant temperature coefficient ($\delta k/k$ per $^{\circ}\text{C}$)	-9.4×10^{-5}
Total fuel, coolant and moderator temperature coefficient ($\delta k/k$ per $^{\circ}\text{C}$)	-2.5×10^{-4}
Total coolant void coefficient ($\delta k/k$ per % void)	-9.1×10^{-4}
Total coolant and moderator void coefficient ($\delta k/k$ per % void)	-5.4×10^{-3}
The prompt neutron lifetime $\bar{\lambda}$ (s)	6.44×10^{-4}

The effective delayed neutron fraction β_{eff}	6.92 x 10 ⁻³
The top reflector worth ($\rho\%$)	9.2
The worth of first 0.2 m of top reflector ($\rho\%$)	6.6

The void and temperature coefficients decreased in magnitude by 4 per cent or less for the lower burnup core, which consisted of 107.78 g elements. The prompt neutron lifetime was about 10 per cent lower and β_{eff} remained unchanged for the low burnup core.

The fuel plus coolant temperature coefficients and the coolant void coefficients are given for each fuel element in Figures 9 and 10 respectively.

7. CONCLUSIONS

The models described in this report are considerably more detailed than earlier models, and include horizontal and vertical heavy water facilities, rigs and safety rod sleeves. The end-of-program reactivity is reasonably well predicted and satisfactory agreement has been achieved with the compilation of experimentally derived parameters. These models have been used to compile operation and safety related parameters such as core position factors, fuel coefficients of reactivity, void coefficients and temperature coefficients.

8. REFERENCES

- Bicevskis, A., Culley, D., Hesse, E. and Wall T. [1967] - A comparison of some measured and calculated reaction rates in HIFAR. AAEC/TM408
- Cawley, R.J. [1983] - UNED - An interactive text editor for the IBM370 computer. AAEC/E580.
- Clancy, B.E. [1982] - A one-dimensional multigroup SN transport theory module for the AUS reactor neutronics system. AAEC/E539.
- Connolly, J.W. and McKenzie, C.D. [1960] - Reactor physics studies on the HIFAR twenty-five element cores. AAEC/TM64.

- Duerden, P. [1973] - HIFAR physics data. AAEC Internal Report O/TN/12.
- Garber, D. [1975] - ENDF/B summary documentation. BNL-17541.
- Harries, J.R. [1978] - Inverse kinetics reactivity measurements on the materials testing reactor HIFAR. AAEC/E456.
- Pollard, J.P. [1974] - AUS module POW - A general purpose 0, 1 and 2D multigroup neutron diffusion code including feedback-free kinetics. AAEC/E269.
- Rhoades, W.A. and Mynatt, F.R. [1973] - The DOT III two-dimensional discrete ordinates transport code. ORNL-TM-4280.
- Robinson, G.S. [1975a] - AUS - The Australian modular scheme for reactor neutronics computations. AAEC/E369.
- Robinson, G.S. [1975b] - AUS burnup module CHAR and the associated status data pool. AAEC/E372.
- Robinson, G.S. [1977] - AUS module MIRANDA - A data preparation code based on multiregion resonance theory. AAEC/E410.

TABLE 1
DATA FOR HIFAR OPERATING PROGRAMS 243-252

Quantity	OP251	Range for OP243-252
Core weight at startup (g)	2652.12	2645 - 2819
Core weight at shutdown (g)	2337.5	2337.5 - 2524
Excess reactivity at startup ($\rho\%$)	7.21	6.74 - 7.52
Excess reactivity at shutdown ($\rho\%$)	1.43	1.0 - 1.67
In-core rig burden ($\rho\%$)	2.3	2.3 - 3.1
Reflector rig burden ($\rho\%$)	1.5*	1.5*

*This value was used in BVHFXYA1, BVHFXYE1 and BVHIFRZ.

A corrected value of $\rho = 2.2\%$ was used in BVHFXYA2 and BVHFXYE2

TABLE 2
REACTIVITY CONTROLLED BY RIGS AND FACILITIES
IN THE AVERAGE FUEL MODELS

Facility	Percentage Reactivity Controlled in	
	BVHFXYA1	BVHFXYA2
10H void only	0.35	0.35
6H and 4H voids only	0.73	0.73
10H, 6H, 4H RAT re-entrant tubes and liners	0.99	0.99
Safety rod Al thimbles and voids + vertical D ₂ O facility Al thimbles	1.45	1.45
In-core rigs	2.16	2.16
Heavy water rigs	1.26	2.07
TOTAL	6.94	7.75

TABLE 3
REACTIVITY CONTROLLED BY RIGS DURING OP251

Rig Position	Updated $\rho\%$ used in BVHFXYA2 and BVHFXYE2	$\rho\%$ used in BVHFXYA1 and BVHFXYE1
6V-1	0.68	0.10
2V-7	0.11	0.16
2V-1	0.05	0.08
2V-2	0.15	0.12
2V-3	0.15	0.19
2V-6	0.12	0.12
6V-3	0.41	0.31
2V-9	0.13	0.13
2V-5	0.11	0.11
2V-4	0.08	0.09
2V-8	0.11	-
4V-4	0.11	0.10
B5	0.38	0.38
C4	0.41	0.41
D3	0.55	0.55
B4	0.43	0.43
C2	0.55	0.55

TABLE 4
 VARIATION OF CELL FLUX SHAPE WITH BURNUP

^{235}U Loading (g)	Burnup Mwd/Element	Thermal Flux Ratio	
		Fuel/CL	Fuel/Cell Ave.
150	0	0.8939	0.8291
149.28	0.575	0.8907	0.8231
135.54	11.493	0.8959	0.8319
121.80	22.450	0.9022	0.8424
107.78	33.683	0.9090	0.8538
93.87	44.869	0.9162	0.8658
80.04	56.038	0.9239	0.8785
67.45	66.247	0.9314	0.8908
56.17	75.439	0.9387	0.9025

TABLE 5
FLUX DEPRESSION IN FUEL CAUSED BY A RIG

Case	Rig Worth $\rho\%$	Thermal Flux Ratio Fuel/Cell Ave.	Fuel Thermal Flux (arbitrary units)	
			Calculated	Culley
Standard HIFAR		0.8662	1.0	1.0
MoO ₃ in HFE in C3	0.95	0.8520	0.930	0.829
UO ₂ in HFE in C3	0.18	0.8606	0.969	0.951
Ir in HFE in C3	0.32	0.8601	0.967	0.919

TABLE 6
FLUX VARIATION WITH BURNUP

²³⁵ U loading in C3 (g)	Core Mass (kg)	CL Thermal Flux (arbitrary units)	CL Epithermal/ Thermal Flux Ratio
135.54	2.47448	1.1309	0.9287
107.78	2.44672	1.1885	0.8638
80.04	2.41898	1.2573	0.7936
56.17	2.39511	1.3296	0.7280

	A1 83.39	A2 77.33	A3 134.08	A4 80.14		
B1 79.86	B2 94.76	B3 114.54	B4 96.68	B5 72.88	B6 80.41	
	C1 83.89	C2 117.60	C3 125.62	C4 129.18	C5 90.68	
D1 80.64	D2 84.96	D3 103.63	D4 114.12	D5 89.48	D6 73.24	
	E1 67.44	E2 74.61	E3 120.21	E4 68.13		

FIGURE 1. END-OF-PROGRAM 251 FUEL LOADING

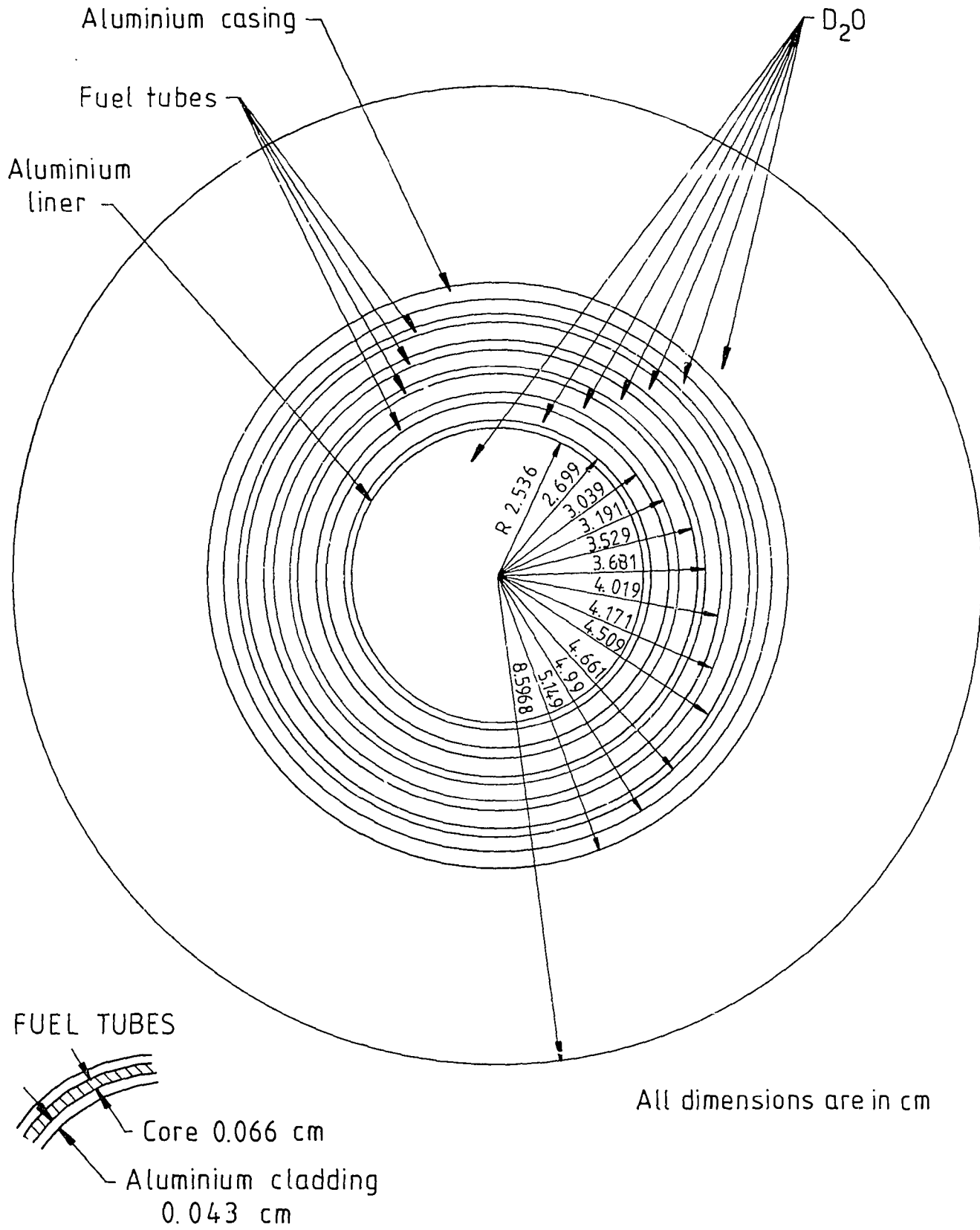


FIGURE 2. BVHIFXS FUEL CELL GEOMETRY

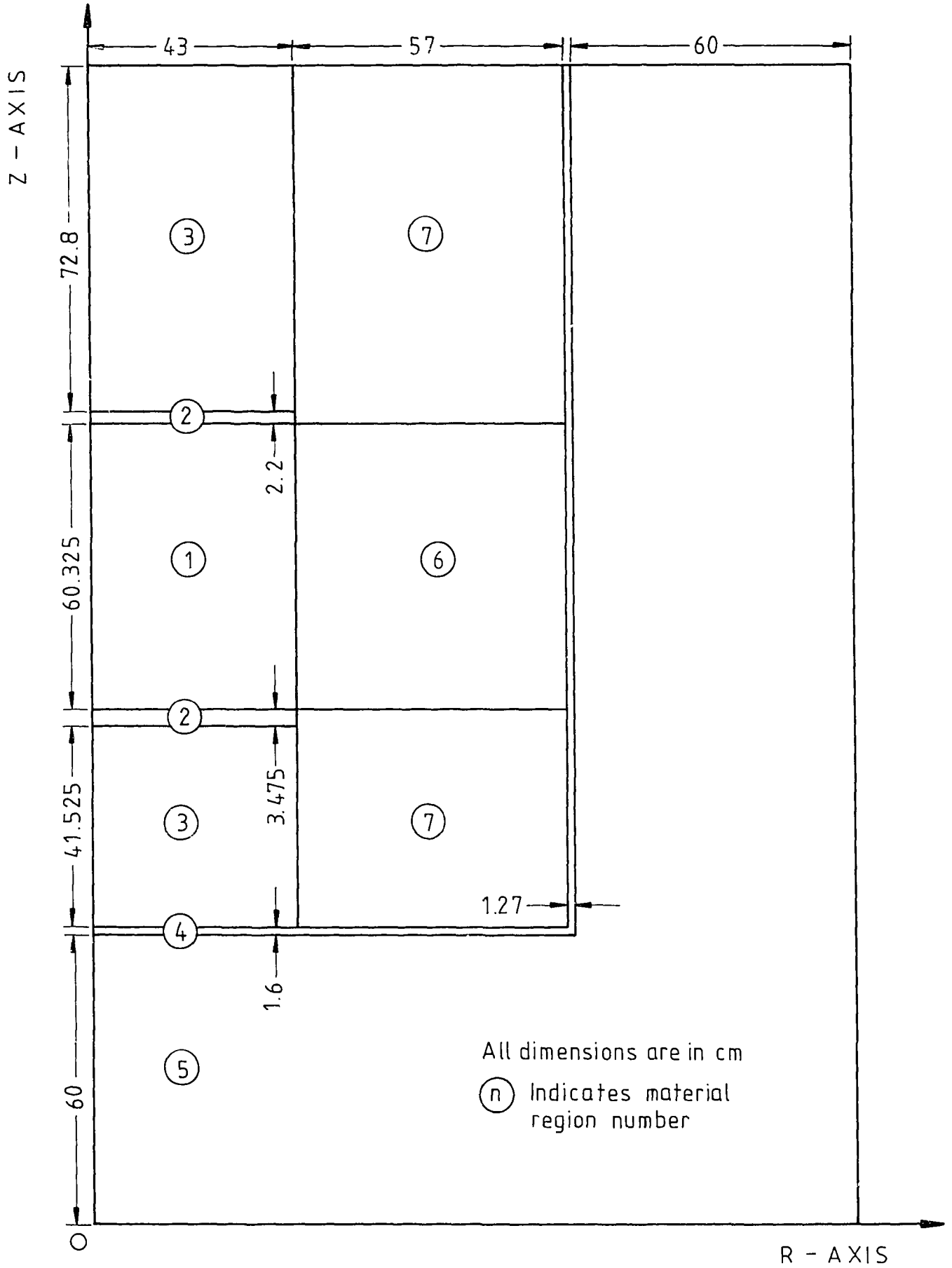


FIGURE 3. BVHIFRZ GEOMETRY

	0.6318	0.6980	0.6887	0.6541	
0.6592	0.7642	0.8582	0.8713	0.7830	0.6982
	0.7930	0.9249	0.9580	0.9257	0.8023
0.7240	0.8029	0.9224	0.9114	0.8168	0.7231
	0.7192	0.7953	0.8195	0.7306	

FIGURE 4. CORE POSITION FACTORS

	-0.8714	-1.1429	-1.1154	-0.9149	
-0.8914	-1.4941	-1.9347	-1.8459	-1.4334	-0.9768
	-1.5016	-2.0659	-2.4182	-2.1037	-1.5314
-1.0553	-1.6379	-2.0533	-2.1724	-1.6964	-1.0553
	-1.1080	-1.4586	-1.5342	-1.1326	

 FIGURE 5. ABSORBER COEFFICIENTS
 ($10^2 \times \rho\%$ per cm^2)

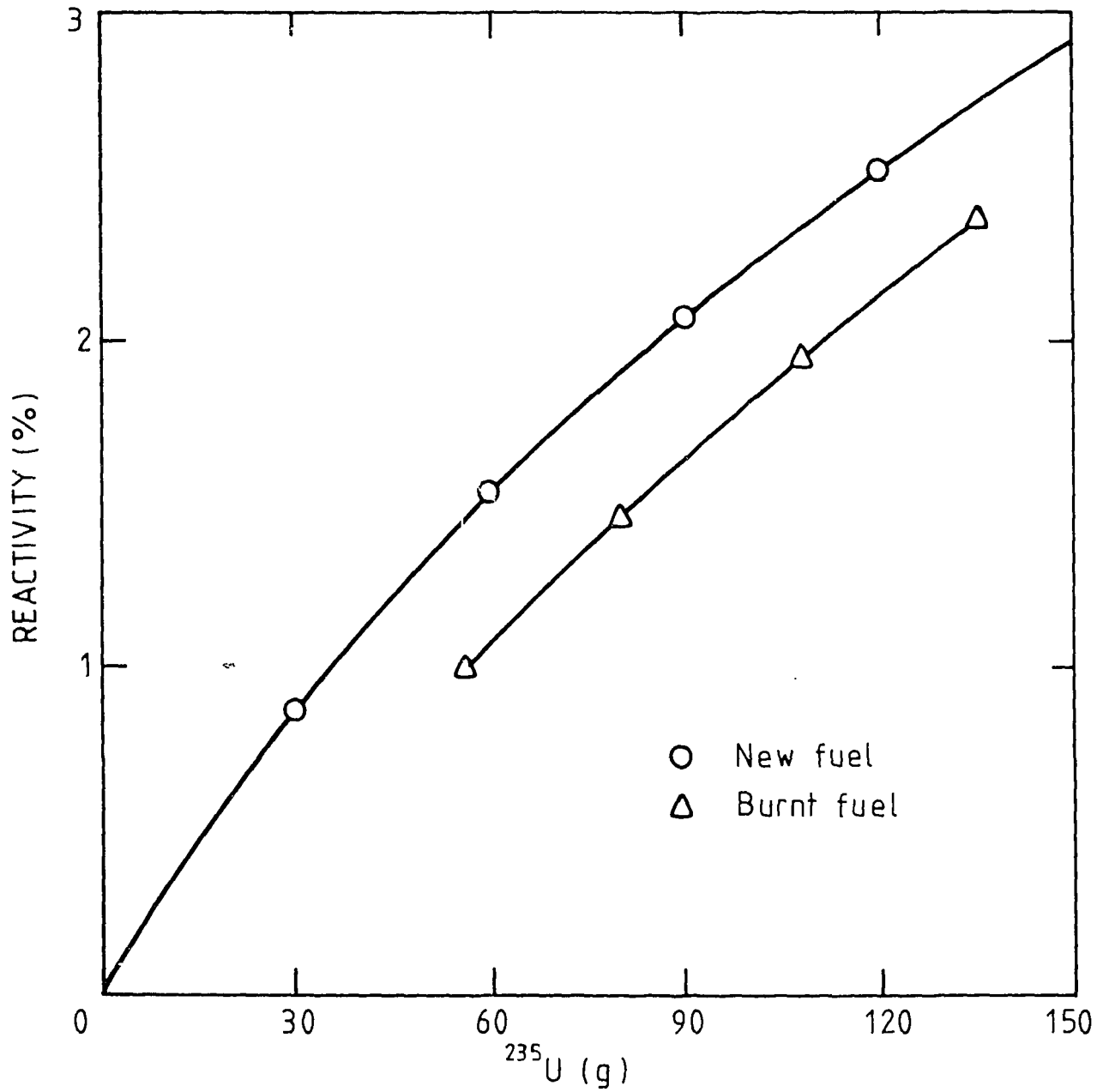


FIGURE 6. REACTIVITY VARIATION WITH CENTRAL ELEMENT FUEL MASS

	-0.00654	-0.00821	-0.00828	-0.00715	
-0.00698	-0.01034	-0.01342	-0.01371	-0.01090	-0.00772
	-0.01079	-0.01528	-0.01712	-0.01536	-0.01107
-0.00814	-0.01158	-0.01519	-0.01500	-0.01167	-0.00813
	-0.00846	-0.01071	-0.01096	-0.00855	

FIGURE 7. FUEL PLUS POISON COEFFICIENTS
($\rho\%$ per g ^{235}U burnup)

	0.621	0.701	0.709	0.611	
0.562	0.802	0.852	0.837	0.785	0.545
	0.731	0.837	0.874	0.840	0.729
0.543	0.800	0.831	0.848	0.793	0.545
	0.604	0.687	0.672	0.589	

FIGURE 8. CELL-AVERAGE, MID-PLANE EPITHERMAL/THERMAL
FLUX RATIOS

	-2.407×10^{-6}	-2.924×10^{-6}	-2.947×10^{-6}	-2.625×10^{-6}	
-2.619×10^{-6}	-3.558×10^{-6}	-4.498×10^{-6}	-4.461×10^{-6}	-3.622×10^{-6}	-2.890×10^{-6}
	-3.767×10^{-6}	-4.924×10^{-6}	-5.673×10^{-6}	-5.003×10^{-6}	-3.872×10^{-6}
-3.044×10^{-6}	-3.973×10^{-6}	-4.915×10^{-6}	-5.026×10^{-6}	-4.015×10^{-6}	-3.042×10^{-6}
	-3.118×10^{-6}	-3.810×10^{-6}	-3.899×10^{-6}	-3.141×10^{-6}	

FIGURE 9. FUEL PLUS COOLANT TEMPERATURE COEFFICIENTS
($\delta k/k$ per $^{\circ}\text{C}$)

	-2.518×10^{-5}	-3.206×10^{-5}	-3.101×10^{-5}	-2.298×10^{-5}	
-2.264×10^{-5}	-3.903×10^{-5}	-4.782×10^{-5}	-4.531×10^{-5}	-3.563×10^{-5}	-2.175×10^{-5}
	-3.574×10^{-5}	-4.870×10^{-5}	-5.565×10^{-5}	-4.986×10^{-5}	-3.601×10^{-5}
-2.393×10^{-5}	-4.018×10^{-5}	-4.863×10^{-5}	-5.164×10^{-5}	-4.269×10^{-5}	-2.448×10^{-5}
	-2.772×10^{-5}	-3.545×10^{-5}	-3.640×10^{-5}	-2.962×10^{-5}	

FIGURE 10. COOLANT VOID COEFFICIENTS
($\delta k/k$ per % void)

APPENDIX A
BVHIFXS, BVHIFCEL, BVHIFRZ AND BVHFXA2 LISTINGS

```
//BVHIFXS JOB ('***/8120000',N1),B.V.HARRINGTON,
// CLASS=J,
// TIME=15
/*ROUTE PRINT PHYS
/*JOBPARM L=8
// EXEC AUS,XS3='BVH.HIFARSF1',DISPXS3=ULD
//GU.SYSIN DD *
*DD1
STEP *
    MODIFY
    LINK MIRANDA(1,7)
    DO 1 1=1,9
    LINK MIRANDA(1,2),(11,29)
    LINK ANAUSN(1,3),(3,99)
    LINK EDIT(1,4),(12,28)
    LINK MERGEL(1,5),(10,28)
    LINK CHAR(1,6),(8,29)
1 CONTINUE
    LINK MERGEL(1,8)
    END

STOP
*DD2
HEAD HIFAR MARK 4/5 1979 STANDARD
TEST -1
TEMP 323
SELECT D2J ENDFB3
SELECT H2U ENDFB3
DEFN A AL .0603
DEFN R1 U235 .9767-3 U238 2.41-4 AL .0592
DEFN R2 U235 .9889-3 U238 2.44-4 AL .0589
DEFN R3 U235 1.005-3 U238 2.48-4 AL .0590
DEFN R4 U235 1.012-3 U238 2.50-4 AL .0588
DEFN D20A D2U .03269 H2O .000267
DEFN D20B D2U .03269 H2O .000267
DEFN CENTRE D20A 1.0
REQD CENTRE A R1 R2 R3 R4 D20A D20B ZZ999
RM 0 4*.634 .1626 .34 .043 .066 .043 .338 .043 .066 .043 .338 .043 .066
    .043 .338 .043 .066 .043 .329 .159 6*.5747 0
REG 1(1)4 CENTRE 5 A 6 D20A 7 A 8 R1 9 A 10 D20A 11 A 12 R2 13 A
14 D20A 15 A 16 R3 17 A 18 D20A 19 A 20 R4 21 A 22 D20A 23 A 24(1)29
D20B
RESREG 0 3.0816 .066 .424 .066 .424 .066 .424 .066 3.9792 0
SMEAR 7*1 2 3*3 4 3*5 6 3*7 8 9*9
GROUPS 25 1 6 11 17 23 29 35 41 47 53 63 71 78 82(2)92 95 99 104 109
    118 124 128
ISOTLIB 11 R1 R2 R3 R4 BURNUP
OUTPUT ZERO AUS GEOM
START
STOP
*DD3
*DD4
OUTPUT AUS GROUPS 5 1 2 5 12 20 25
SEARCH ON BSQ FOR 1.03
REQD -1 ZZ999 CELL,0
START
OUTPUT RRM
WHERE @MIDPT=1
WHERE @FUELMAT=8,12,16,20
WHERE @EDGE=29
```

(Continued)

```

DEFN MIDPT=ZZ9999MIDPT
DEFN FUELMAT=ZZ9999FUELMAT
DEFN AVE=ZZ9999AVE
DEFN EDGE=ZZ9999EDGE
DEFN R1Z=ZZ9999R1
DEFN R2Z=ZZ9999R2
DEFN R3Z=ZZ9999R3
DEFN R4Z=ZZ9999R4
REQD MIDPT R1Z R2Z R3Z R4Z EDGE FUELMAT AVE R1 R2 R3 R4
START
STOP
*DD5
HIFAR
12 10 12 0
*DD6
FLUX DENSITY 1.17E14 FOR $FUEL GRPS 15 TO 25
STEP 1
XSLIB 8
HEIGHT 60.325
FOLLOW 6 U235 U238 PU239 PU240 PU241 PU242
AVERAGE 1 $FUEL $ALL
START
*DD8
HIFAR
12 0 12 14 1(1)3 6(2)22 4 5 14*1
*DD10
STEP 20
STEP 22
STEP 25
STEP 28
STEP 32
STEP 34
STEP 36
*DD7
HEAD REFL
TEMP 323
SELECT D2O ENDFB3
SELECT H2O ENDFB3
SELECT C ENDFB4 ORIG
GROUPS 5 1 11 29 79 99 129
DEFN GRAPH C .0803
REQD GRAPH
RM 0 1 0
REG 1 GRAPH
RESREG
STATOFF
OUTPUT 12
START
DEFN D2OR D2O .03269 H2O .000267
DEFN ALR AL .0603
DEFN SST304 FE .063 CR .01567 NI 6.858-3 MN 6.54-4 SI 7.68-4
REQD D2OR ALR SST304
REG 1 D2OR
OUTPUT 12
START
STOP
/*
//

```

MUD

MUD

MUD

MUD

MUD

MUD

MUD

```
//BVHIFCEL JOB ('*****/8120000',N1),B.V.HARRINGTON,
// CLASS=5,
```

```
// TIME=5
```

```
/*ROUTE PRINT PHYS
```

```
/*JOBPARM L=2
```

```
// EXEC AUS
```

```
//GO.SYSIN DD *
```

```
*DD1
```

```
STEP *
```

```
LINK MIRANDA(1,7)
```

```
LINK MIRANDA(1,2),(11,29)
```

```
LINK ANAUSN(1,3),(3,99)
```

```
LINK EDIT(1,4),(12,28)
```

```
LINK MERGEL(1,5),(10,28)
```

```
END
```

```
STOP
```

```
*DD2
```

```
HEAD HIFAR MARK 4/5 1979 STANDARD
```

```
TEST -1
```

```
TEMP 323
```

```
SELECT D2J ENDFB3
```

```
DEFN A AL .0603
```

```
DEFN R196
```

U235	6.16759E-04U236	5.72811E-05NP237	9.19873E-07U238	2.35886E-04
PU238	5.44356E-08PU239	3.08299E-06PU240	4.81551E-07PU241	1.31251E-07
PU242	1.11640E-08AM241	4.32532E-10AM242M	3.41436E-12AM243	2.64232E-10
CM242	5.38669E-11CM243	2.08168E-13CM244	9.85366E-12CM245	7.26430E-14
AL	5.92000E-02KR83	1.48069E-06ZR95	1.19500E-05NB95	4.21747E-06
MU95	3.50951E-06TC99	1.81933E-05RU100	4.16253E-07RU101	1.54458E-05
RU102	1.28365E-05RU103	4.38743E-06RH103	4.81414E-06RH105	4.72171E-08
PD104	3.69967E-07PD105	2.50904E-06PD106	1.73603E-06PD107	3.59364E-07
PD108	2.17190E-07AG109	9.87689E-08CD113	1.09603E-09XE131	7.86405E-06
XE133	1.33911E-06XE135	7.10794E-09CS133	1.84155E-05CS134	4.43451E-07
CS135	1.59472E-06CE144	1.43968E-05PR143	3.14815E-06ND143	1.32542E-05
ND144	3.45760E-06ND145	1.15832E-05ND146	9.25645E-06ND147	9.84785E-07
ND148	5.14021E-06PM147	5.02160E-06PM148M	3.68965E-08PM148	4.47657E-08
PM149	1.11373E-07SM147	1.63340E-07SM149	6.37009E-08SM150	3.33620E-06
SM151	1.78942E-07SM152	1.73022E-06EU153	6.94082E-07EU154	1.00689E-07
EU155	4.92837E-08GD157	1.35773E-10FPF	3.90367E-04	

```
DEFN R296
```

U235	6.26699E-04U236	5.76428E-05NP237	9.19421E-07U238	2.38946E-04
PU238	5.41960E-08PU239	3.05451E-06PU240	4.74222E-07PU241	1.29364E-07
PU242	1.09326E-08AM241	4.26804E-10AM242M	3.36451E-12AM243	2.58440E-10
CM242	5.28715E-11CM243	2.03598E-13CM244	9.58346E-12CM245	7.05775E-14
AL	5.89000E-02KR83	1.49036E-06ZR95	1.20265E-05NB95	4.24047E-06
MU95	3.52600E-06TC99	1.83019E-05RU100	4.16718E-07RU101	1.55364E-05
RU102	1.29109E-05RU103	4.41620E-06RH103	4.84029E-06RH105	4.76387E-08
PD104	3.70189E-07PD105	2.52599E-06PD106	1.74125E-06PD107	3.60610E-07
PD108	2.17886E-07AG109	9.90526E-08CD113	1.10921E-09XE131	7.91298E-06
XE133	1.35051E-06XE135	7.20910E-09CS133	1.85238E-05CS134	4.43877E-07
CS135	1.61385E-06CE144	1.44833E-05PR143	3.17310E-06ND143	1.33380E-05
ND144	3.46403E-06ND145	1.16530E-05ND146	9.30921E-06ND147	9.92722E-07
ND148	5.16999E-06PM147	5.05313E-06PM148M	3.70974E-08PM148	4.48785E-08
PM149	1.12155E-07SM147	1.64213E-07SM149	6.44417E-08SM150	3.35391E-06
SM151	1.81963E-07SM152	1.73933E-06EU153	6.96942E-07EU154	1.00648E-07
EU155	4.95687E-08GD157	1.37753E-10FPF	3.92650E-04	

```
DEFN R396
```

U235	6.31225E-04U236	5.93897E-05NP237	9.51762E-07U238	2.42818E-04
PU238	5.67683E-08PU239	3.11094E-06PU240	4.89544E-07PU241	1.33841E-07

(Continued)

PU242	1.15276E-08AM241	4.41597E-10AM242M	3.49262E-12AM243	2.73869E-10
CM242	5.54707E-11CM243	2.15588E-13CM244	1.02814E-11CM245	7.58609E-14
AL	5.90000E-02KR83	1.53652E-06ZR95	1.24036E-05NB95	4.38323E-06
MU95	3.65118E-06TC99	1.88948E-05RU100	4.34264E-07RU101	1.60426E-05
RU102	1.33325E-05RU103	4.55129E-06RH103	5.00192E-06RH105	4.87384E-08
PD104	3.87356E-07PD105	2.60043E-06PD106	1.80690E-06PD107	3.72523E-07
PD108	2.25116E-07AG109	1.02288E-07CD113	1.12164E-09XE131	8.16415E-06
XE133	1.38576E-06XE135	7.27241E-09CS133	1.91274E-05CS134	4.62939E-07
CS135	1.03646E-06CE144	1.49513E-05PR143	3.26083E-06ND143	1.37564E-05
ND144	3.61344E-06ND145	1.20289E-05ND146	9.61700E-06ND147	1.01983E-06
ND148	5.33932E-06PM147	5.21405E-06PM148M	3.81773E-08PM148	4.66495E-08
PM149	1.15454E-07SM147	1.69809E-07SM149	6.53005E-08SM150	3.46767E-06
SM151	1.83440E-07SM152	1.79851E-06EU153	7.21896E-07EU154	1.05401E-07
EU155	5.10469E-03GD157	1.38494E-10FP	4.05451E-04	
DEFN R496				
U235	6.21221E-04U236	6.18424E-05NP237	1.00792E-06U238	2.44558E-04
PU238	6.18379E-08PU239	3.21586E-06PU240	5.22383E-07PU241	1.44258E-07
PU242	1.30363E-08AM241	4.76735E-10AM242M	3.80406E-12AM243	3.13566E-10
CM242	6.20308E-11CM243	2.46660E-13CM244	1.21483E-11CM245	9.00777E-14
AL	5.88000E-02KR83	1.60124E-06ZR95	1.29384E-05NB95	4.59819E-06
MU95	3.84756E-06TC99	1.97601E-05RU100	4.65376E-07RU101	1.67854E-05
RU102	1.39531E-05RU103	4.73929E-06RH103	5.24446E-06RH105	4.98589E-08
PD104	4.18757E-07PD105	2.70112E-06PD106	1.91573E-06PD107	3.91121E-07
PD108	2.36494E-07AG109	1.07383E-07CD113	1.11755E-09XE131	8.52435E-06
XE133	1.42686E-06XE135	7.19401E-09CS133	2.00126E-05CS134	4.96965E-07
CS135	1.64039E-06CE144	1.56327E-05PR143	3.37025E-06ND143	1.43504E-05
ND144	3.87686E-06ND145	1.25755E-05ND146	1.00739E-05ND147	1.05316E-06
ND148	5.58894E-06PM147	5.44482E-06PM148M	3.96974E-08PM148	4.96440E-08
PM149	1.19884E-07SM147	1.78307E-07SM149	6.53889E-08SM150	3.63994E-06
SM151	1.80855E-07SM152	1.88767E-06EU153	7.61485E-07EU154	1.14205E-07
EU155	5.31962E-08GD157	1.36076E-10FP	4.24250E-04	
DEFN R1128				
U235	5.27195E-04U236	7.09003E-05NP237	1.41344E-06U238	2.34495E-04
PU238	1.09659E-07PU239	3.36904E-06PU240	6.80023E-07PU241	2.23726E-07
PU242	2.72018E-08AM241	1.00713E-09AM242M	8.79325E-12AM243	8.25955E-10
CM242	1.67967E-10CM243	8.32661E-13CM244	4.13288E-11CM245	3.62573E-13
AL	5.92000E-02KR83	1.79918E-06ZR95	1.26929E-05NB95	5.36220E-06
MU95	6.53111E-06TC99	2.26122E-05RU100	6.74987E-07RU101	1.93020E-05
RU102	1.61006E-05RU103	4.34566E-06RH103	6.91668E-06RH105	4.14130E-08
PD104	7.28739E-07PD105	3.16040E-06PD106	2.20866E-06PD107	4.62409E-07
PD108	2.80531E-07AG109	1.26476E-07CD113	9.70567E-10XE131	9.62732E-06
XE133	1.16313E-06XE135	6.06646E-09CS133	2.33412E-05CS134	7.35012E-07
CS135	1.99381E-06CE144	1.72397E-05PR143	2.75866E-06ND143	1.69402E-05
ND144	5.90970E-06ND145	1.43760E-05ND146	1.17005E-05ND147	8.59645E-07
ND148	6.43132E-06PM147	6.22797E-06PM148M	4.44252E-08PM148	5.45643E-08
PM149	1.05021E-07SM147	2.87028E-07SM149	5.94482E-08SM150	4.34529E-06
SM151	1.67348E-07SM152	2.15873E-06EU153	9.39747E-07EU154	1.65710E-07
EU155	6.34674E-08GD157	1.18014E-10FP	4.88446E-04	
DEFN R2128				
U235	5.36228E-04U236	7.14087E-05NP237	1.41189E-06U238	2.37569E-04
PU238	1.09159E-07PU239	3.34055E-06PU240	6.70706E-07PU241	2.20470E-07
PU242	2.66399E-08AM241	9.93504E-10AM242M	8.66736E-12AM243	8.09341E-10
CM242	1.64908E-10CM243	8.15112E-13CM244	4.02632E-11CM245	3.52894E-13
AL	5.89000E-02KR83	1.81277E-06ZR95	1.27890E-05NB95	5.39653E-06
MU95	6.56572E-06TC99	2.27662E-05RU100	6.76166E-07RU101	1.94308E-05
RU102	1.62064E-05RU103	4.37983E-06RH103	6.95991E-06RH105	4.18335E-08
PD104	7.29716E-07PD105	3.18383E-06PD106	2.21677E-06PD107	4.64117E-07
PD108	2.81475E-07AG109	1.26852E-07CD113	9.82832E-10XE131	9.69618E-06
XE133	1.17496E-06XE135	6.15895E-09CS133	2.34988E-05CS134	7.36287E-07
CS135	2.01845E-06CE144	1.73588E-05PR143	2.78530E-06ND143	1.70661E-05
ND144	5.92527E-06ND145	1.44749E-05ND146	1.17759E-05ND147	8.68045E-07

```

ND148 6.47374E-06PM147 6.27395E-06PM148M 4.47100E-08PM148 5.47687E-08
PM149 1.05870E-07SM147 2.88784E-07SM149 6.01718E-08SM150 4.37153E-06
SM151 1.70124E-07SM152 2.17277E-06EU153 9.44335E-07EU154 1.65853E-07
EU155 6.37417E-08GD157 1.19736E-10PFP 4.91694E-04
DEFN R3128
U235 5.38735E-04J236 7.34392E-05NP237 1.45994E-06U238 2.41408E-04
PU238 1.14126E-07PU239 3.39795E-06PU240 6.90751E-07PU241 2.27512E-07
PU242 2.80012E-08AM241 1.02538E-09AM242M 8.96334E-12AM243 8.55159E-10
CM242 1.72519E-10CM243 8.60182E-13CM244 4.30667E-11CM245 3.77950E-13
AL 5.90000E-02KR83 1.86429E-06ZR95 1.31528E-05NB95 5.56564E-06
MO95 6.78921E-06TC99 2.34562E-05RU100 7.03612E-07RU101 2.00245E-05
RU102 1.67034E-05RU103 4.49895E-06RH103 7.17765E-06RH105 4.26403E-08
PD104 7.62202E-07PD105 3.27154E-06PD106 2.29566E-06PD107 4.78592E-07
PD108 2.90308E-07AG109 1.30747E-07CD113 9.91379E-10XE131 9.98148E-06
XE133 1.20058E-06XE135 6.19755E-09CS133 2.42141E-05CS134 7.66535E-07
CS135 2.04513E-06CE144 1.78811E-05PR143 2.85009E-06ND143 1.75540E-05
ND144 6.16967E-06ND145 1.49110E-05ND146 1.21433E-05ND147 8.87945E-07
ND148 6.67274E-06PM147 6.45703E-06PM148M 4.59146E-08PM148 5.67715E-08
PM149 1.08685E-07SM147 2.98094E-07SM149 6.08994E-08SM150 4.51152E-06
SM151 1.71515E-07SM152 2.24030E-06EU153 9.76252E-07EU154 1.73160E-07
EU155 6.58486E-08GD157 1.20200E-10PFP 5.06734E-04
DEFN R4128
U235 5.26878E-04J236 7.61165E-05NP237 1.54338E-06U238 2.43079E-04
PU238 1.23833E-07PU239 3.50088E-06PU240 7.32722E-07PU241 2.43319E-07
PU242 3.13680E-08AM241 1.09843E-09AM242M 9.65577E-12AM243 9.70872E-10
CM242 1.91276E-10CM243 9.74336E-13CM244 5.04617E-11CM245 4.44549E-13
AL 5.88000E-02KR83 1.93083E-06ZR95 1.36231E-05NB95 5.80555E-06
MO95 7.12890E-06TC99 2.44063E-05RU100 7.51214E-07RU101 2.08494E-05
RU102 1.73973E-05RU103 4.64649E-06RH103 7.48751E-06RH105 4.32315E-08
PD104 8.20254E-07PD105 3.38285E-06PD106 2.42194E-06PD107 5.00518E-07
PD108 3.03836E-07AG109 1.36712E-07CD113 9.82072E-10XE131 1.03634E-05
XE133 1.22333E-06XE135 6.09239E-09CS133 2.52030E-05CS134 8.19110E-07
CS135 2.04602E-06CE144 1.85954E-05PR143 2.91432E-06ND143 1.81891E-05
ND144 6.58878E-06ND145 1.55084E-05ND146 1.26630E-05ND147 9.07224E-07
ND148 6.95074E-06PM147 6.69902E-06PM148M 4.74843E-08PM148 5.99356E-08
PM149 1.12090E-07SM147 3.11602E-07SM149 6.07928E-08SM150 4.71420E-06
SM151 1.69134E-07SM152 2.33485E-06EU153 1.02483E-06EU154 1.86186E-07
EU155 6.91617E-08GD157 1.17730E-10PFP 5.27654E-04
DEFN R1 R1128 .0262035 R196 .9737965
DEFN R2 R2128 .0262035 R296 .9737965
DEFN R3 R3128 .0262035 R396 .9737965
DEFN R4 R4128 .0262035 R496 .9737965
DEFN D20A D20 .03269 H20 .000267
DEFN D20B D20 .03269 H20 .000267
DEFN CENTRE D20A 1.0
REQD CENTRE A R1 R2 R3 R4 D20A D20B ZZ999
RM 0 4*.634 .1626 .34 .043 .066 .043 .338 .043 .066 .043 .338 .043
.066 .043 .338 .043 .066 .043 .329 .159 6*.5747 0
REG 1(1)4 CENTRE 5 A 6 D20A 7 A 8 R1 9 A 10 D20A 11 A 12 R2 13 A
14 D20A 15 A 16 R3 17 A 18 D20A 19 A 20 R4 21 A 22 D20A 23 A 24(1)29
D20B
RESREG 0 3.0816 .066 .424 .066 .424 .066 .424 .066 3.9792 0
SMEAR 7*1 2 3*3 4 3*5 6 3*7 8 9*9
GROUPS 25 1 6 11 17 23 29 35 41 47 53 63 71 78 82(2)92 95 99 104 109
118 124 128
OUTPUT ZERO AUS GEOM
START
STOP
*DD3
*DD4
PRINT 1

```

(Continued)

```

OUTPUT AUS GROUPS 5 1 2 5 12 20 25
SEARCH UN BSQ FOR 1.03
REQD -1 ZZ999 CELL,0
START
OUTPUT RRM
WHERE @MIDPT=1
WHERE @FUELMAT=8,12,16,20
WHERE @EDGE=29
DEFN MIDPT=ZZ999@MIDPT
DEFN FUELMAT=ZZ999@FUELMAT
DEFN AVE=ZZ999@AVE
DEFN EDGE=ZZ999@EDGE
DEFN R1Z=ZZ999@R1
DEFN R2Z=ZZ999@R2
DEFN R3Z=ZZ999@R3
DEFN R4Z=ZZ999@R4
REQD MIDPT R1Z R2Z R3Z R4Z EDGE FUELMAT AVE R1 R2 R3 R4
START
STOP
*DD5
HIFAR
12 10 12 0
*DD7
HEAD REFL
TEMP 323
SELECT D2J ENDFB3
GROUPS 5 1 11 29 78 99 128
DEFN GRAPH C .0803
REQD GRAPH
RM 0 1 0
REG 1 GRAPH
RESREG
STATJFF
OUTPUT 12
START
DEFN D2OR D2J .03269 H2O .000267
DEFN ALR AL .0603
DEFN SST304 FE .063 CR .01567 NI 6.858-3 MN 6.54-4 SI 7.68-4
REQD D2OR ALR SST304
REG 1 D2OR
OUTPUT 12
START
STOP
/*
//

```

```

//BVHIFRZ JOB ('*****/81200000',N1),B.V.HARRINGTON,
// CLASS=3,TIME=10
/*RUJTE PRINT PHYS
/*JOBPARM L=2
// EXEC AUS,XS1='BVH.HIFARSF1',DISPXS1=OLD,
// FL1='BVH.HIFLUX',DISPFL1=OLD,
// REGION.GU=500K
//GU.SYSIN DD *
*DD1
STEP *
    LINK POW
    END

STOP
*DD2
PRELUDE MAXX=33,MAXY=48,MAXG=5,MAXM=12,,END
XSD M(1) XSD M(2) XSD M(3) XSD M(9) XSD M(10)
READ LIB ON 10
DEFN FUEL M(4)=M(9) .9737965 M(10) .0262035
DEFN M(5)=M(2) .902 M(3) .098
DEFN M(6)=M(2) .973 M(3) .022
DEFN M(12)=M(2) .99466 M(3) .01534
DEFN M(7)=M(2) .91239 M(3) .03761
DEFN M(8)=M(4)
DEFN M(9)=M(7)
DEFN M(10)=M(3)
DEFN M(11)=M(1)
RM 0 9*4 3 2 2 2 2 3 10*5 1.27 6*10 .71
ZM .71 6*10 1.6 6.525 7*5 2*1.7375 2.1625 3 10*5 3 2.1625 2.2 2.8 14*5
.71
REG MR 1(1)32 MZ 1(1)47 M(1)
REG MR 1(1)26 MZ 7(1)47 M(3)
REG MR 13(1)25 MZ 3(1)47 M(2)
REG MR 1(1)12 MZ 3(1)47 M(6)
REG MR 1(1)12 MZ 13(1)31 M(4)
REG MR 13(1)25 MZ 3(1)47 M(12)
REG MR 13(1)25 MZ 13(1)31 M(7)
REG MR 1(1)12 MZ 16,17,32 M(5)
REG MR 1(1)12 MZ 24,25 M(8)
REG MR 13(1)25 MZ 24,25 M(9)
REG MR 26 MZ 24,25 M(10)
REG MR 27(1)32 MZ 24,25 M(11)
POWER=1.E+7,3
OUTPUT UEDIT
START
GROUPS 5 1,1(1)5
LX 32 1(1)33
LY 3 1,18,32,48
EDITS -1 0 0 0
GROUPS 5 1,1(1)5
LX 32 1(1)33
LY 3 1,24,26,48
EDITS -1 0 0 0
GBSQ 0.2 BSQ(1) 1(1)12 1(1)12 12*0
SEARCH(1.01) *AKEFF WSEA 7*0 4*1 0
ZM 0 2 0
REG MR 1(1)12 M(3) MR 13(1)25 M(9) MR 26 M(10) MR 27(1)32 M(11)
START
STOP
/*

```

(Continued)

```

//BVHFXA2 JJB ('***/8120000',N1),B.V.HARRINGTON,
//          CLASS=4,
//          TIME=4
/*JUBPARM L=4
/*ROUTE PRINT PHYS
// EXEC AUS,XS3='BVH.HIFARF1',DISPXS3=SHR,
// FL1='BVH.HIFARFL',DISPFL1=OLD,REGION.GO=715K
//GU.SYSIN DD *
*DD1
STEP POW
*DD2
PRELUDE MAXG=5 MAXI=33 MAXX=59 MAXY=59 MAXS=4
  END
POW NEWRIGS1 END JF PROGRAM 251 (AVERAGE FUEL LOADING)
XSD M(1) XSD M(2) XSD M(3) XSD M(4)
XSD M(9) XSD M(10) XSD SST304 M(11)
* Z2999 IS A 1/V ABSORBER (WITH 2200 MSEC-1 VALUE OF 1 BARN)
* WHICH HAS BEEN GROUP COLLAPSED OVER A FUEL CELL SPECTRUM.
XSD Z2999 M(33)
* INV455B IS A 1/V ABSORBER (WITH 2200 MSEC-1 VALUE OF 455 BARNS)
* WHICH HAS BEEN GROUP COLLAPSED OVER THE REFLECTOR SPECTRUM.
XSD INV455B M(32)
READ LIB UN 18
DEFN FUEL M(4)=M(3) .9737965 M(10) .0262035
GBSQ
1.20846-3 1.19089-4 9.39771-4 2.14518-4 2.06882-4
6.98216-4 8.23306-4 1.05038-3 5.54614-4 4.14717-4
1.22156-3 1.21636-3 1.05099-3 2.23386-4 2.08549-4
6.40719-4 7.35596-4 9.73960-4 8.00151-4 5.82225-4
BSQ(0) 1(1)4 1(1)4 4*0
BSQ(2) 1(1)4 1(1)4 4*0
DEFN BEAM10H M(5)=M(2) .65
DCX(5) 7.0234 3.55122 3.85526 3.07852 2.40442
DCY(5) 7.0234 3.55122 3.85526 3.07852 2.40442
DEFN F4H34H4 M(6)=M(5) 1. M(3) .054 M(11) .007
DEFN F4H14H2 M(7)=M(5) 1. M(3) .107
DEFN F6H M(8)=M(5) 1. M(3) .1001 M(11) .011
DEFN F6HEND M(10)=M(3) .0972 M(11) .0104 M(5) .8924
DEFN F4H54H6 M(12)=M(5) 1. M(3) .091 M(11) .01
DEFN F6V1 M(13)=M(3) .136 M(2) .864 M(32) 2.86426-5
DEFN F6V2 M(14)=M(3) .136 M(2) .864
DEFN F6V3 M(15)=M(3) .136 M(2) .864 M(32) 2.37156-5
DEFN F6V4 M(16)=M(3) .136 M(2) .864
DEFN F4V1 M(17)=M(3) .181 M(2) .819
DEFN F4V2 M(18)=M(3) .181 M(2) .819
DEFN F4V3 M(19)=M(3) .181 M(2) .819
DEFN F4V4 M(20)=M(3) .181 M(2) .819 M(32) 1.62503-4
DEFN F4V5 M(21)=M(3) .181 M(2) .819
DEFN F2V1 M(22)=M(3) .3039 M(2) .696 M(32) 2.82247-5
DEFN F2V2 M(23)=M(3) .3039 M(2) .696 M(32) 5.97482-5
DEFN F2V3 M(24)=M(3) .355 M(2) .645 M(32) 3.53467-5
DEFN F2V4 M(25)=M(3) .3039 M(2) .696 M(32) 4.12783-5
DEFN F2V5 M(26)=M(3) .199 M(2) .801 M(32) 3.43772-5
DEFN F2V6 M(27)=M(3) .3039 M(2) .696 M(32) 7.98524-5
DEFN F2V7 M(28)=M(3) .3039 M(2) .696 M(32) 4.37340-5
DEFN F2V8 M(29)=M(3) .355 M(2) .645 M(32) 2.40300-5
DEFN F2V9 M(30)=M(3) .3039 M(2) .696 M(32) 5.61774-5
DEFN SR0D M(31)=M(3) .197 M(2) .6056
DEFN FUELBS M(34)=M(4) 1. M(32) 3.3313-6

```

DEFN FUELC4 M(35)=M(4) 1. M(32) 2.6083-6
 DEFN FUEL D3 M(36)=M(4) 1. M(32) 3.5439-6
 DEFN FUELB4 M(37)=M(4) 1. M(32) 3.0828-6
 DEFN FUELC2 M(38)=M(4) 1. M(32) 3.5894-6
 DEFN F10HEND M(9)=M(3) .2196 M(11) .0286 M(5) .7518
 DEFN F10H M(5)=M(5) 1. M(3) .0646 M(11) .00873
 DEFN ALD2J M(3)=M(3) .2134 M(2) .7952
 XM .71 6*10. 10*5. 4.28 24*3.81 4.28 10*5. 6*10. .71
 YM .71 6*10. 10*5. 4.28 24*3.81 4.28 10*5. 6*10. .71
 REG MX 1(1)58 MY 1(1)58 M(1)
 REG MX 7,52 MY 23(1)36 M(3)
 REG MX 23(1)36 MY 7,52 M(3)
 REG MX 8 51 MY 18(1)41 M(3)
 REG MX 18(1)41 MY 3,51 M(3)
 REG MX 9,50 MY 17(1)42 M(3)
 REG MX 17(1)42 MY 9 50 M(3)
 REG MX 10,49 MY 15(1)44 M(3)
 REG MX 15(1)44 MY 10,49 M(3)
 REG MX 11,48 MY 14(1)45 M(3)
 REG MX 14(1)45 MY 11 48 M(3)
 REG MX 12 47 MY 12(1)47 M(3)
 REG MX 12(1)47 MY 12 47 M(3)
 REG MX 24(1)35 MY 3(1)51 M(2)
 REG MX 8(1)51 MY 24(1)35 M(2)
 REG MX 19(1)23 36(1)40 MY 9(1)50 M(2)
 REG MX 9(1)50 MY 19(1)23 36(1)40 M(2)
 REG MX 18 41 MY 10(1)49 M(2)
 REG MX 10(1)49 MY 18 41 M(2)
 REG MX 16 17 42 43 MY 11(1)48 M(2)
 REG MX 11(1)48 MY 16 17 42 43 M(2)
 REG MX 15 44 MY 12(1)47 M(2)
 REG MX 12(1)47 MY 15 44 M(2)
 REG MX 13 14 45 46 MY 13(1)46 M(2)
 REG MX 22(1)37 MY 20(1)39 M(4)
 REG MX 18(1)21 38(1)41 MY 24(1)27 32(1)35 M(4)
 REG MX 20 21 38 39 MY 28(1)31 M(4)
 REG MX 13(1)19 MY 40(1)46 M(5)
 REG MX 15(1)19 MY 39 4(5)
 REG MX 20 MY 40(1)44 4(5)
 REG MX 17 18 MY 38 M(5)
 REG MX 21 MY 41 42 M(5)
 REG MX 28(1)31 MY 41(1)49 M(6)
 REG MX 13,14 MY 13,14 M(12)
 REG MX 14,15 MY 14,15 M(12)
 REG MX 15,16 MY 15,16 M(12)
 REG MX 16,17 MY 16,17 M(12)
 REG MX 16 MY 18 M(12)
 REG MX 18 MY 16 M(12)
 REG MX 41 MY 43 M(7)
 REG MX 43 MY 41 M(7)
 REG MX 42,43 MY 42,43 M(7)
 REG MX 43 44 MY 43 44 M(7)
 REG MX 44 45 MY 44 45 M(7)
 REG MX 45 46 MY 45 46 M(7)
 REG MX 38 MY 19 20 M(10)
 REG MX 39 40 MY 21 M(10)
 REG MX 39,40 MY 19(1)20 M(8)
 REG MX 40(1)42 MY 17(1)19 M(8)
 REG MX 42(1)44 MY 15(1)17 M(8)
 REG MX 44(1)46 MY 13(1)15 M(8)
 REG MX=18 MY=38 M(9)

(Continued)

```

REG MX=19 MY=39 M(9)
REG MX=20 MY=40 M(9)
REG MX=21 MY=41 M(9)
REG MX 23(1)26 MY 15(1)17 M(13)
REG MX 23(1)26 MY 42(1)44 M(14)
REG MX 33(1)36 MY 42(1)44 M(15)
REG MX 33(1)36 MY 15(1)17 M(16)
REG MX 23,24 MY 10,11 M(17)
REG MX 24,25 MY 48,49 M(18)
REG MX 35,36 MY 48,49 M(19)
REG MX 46,47 MY 17,18 M(20)
REG MX 35,36 MY 10,11 M(21)
REG MX 15 MY 22 M(22)
REG MX 15 MY 26 M(23)
REG MX 17 MY 30 M(24)
REG MX 15 MY 34 M(25)
REG MX 19 MY 37,38 M(26)
REG MX 44 MY 37 M(27)
REG MX 44 MY 33 M(28)
REG MX 42 MY 29 M(29)
REG MX 44 MY 25 M(30)
REG MX 19,20 MY 21,22 M(31)
REG MX 39,40 MY 37,38 M(31)
REG MX 34(1)37 MY 32(1)35 M(34)
REG MX 32(1)35 MY 23(1)31 M(35)
REG MX 26(1)29 MY 24(1)27 M(36)
REG MX 30(1)33 MY 32(1)35 M(37)
REG MX 24(1)27 MY 28(1)31 M(38)
* POWER=(POWER/CM)*(PEAK THERMAL FLUX/AVE THERMAL FLUX)
*      =1.6576875E+5*1.044
* RESULTING FLUXES ARE CENTRE PLANE FLUXES.
POWER=1.7306257E+5,3
OUTPUT UEDIT
RESTART
* POWER
GROUPS 1 1,5
LX 3 1,18,42,59
LY 3 1,20,40,59
EDITS -1 3 2 0
GROUPS 1 1,5
LX 8 1,18(4)42,59
LY 7 1,20(4)40,59
EDITS -1 3 2 0
GROUPS 1 1,5
LX 7 1,20(4)40,59
LY 3 1,28,32,59
EDITS -1 3 2 0
* 5 GROUP FLUXES
GROUPS 5 1,1(1)5
LX 7 1,20(4)40,59 LY 3 1,28,32,59
EDITS -2 1 0 0
GROUPS 5 1,1(1)5
LX 8 1,18(4)42,59
LY 7 1,20(4)40,59
EDITS -2 1 0 0
* 1/V FLUX
GROUPS 1 1,5 MXS 38*33
LX 7 1,20(4)40,59 LY 3 1,28,32,59
EDITS -3 -2 -1 0
GROUPS 1 1,5 MXS 38*33
LX 8 1,18(4)42,59

```

```
LY 7 1,20(4)40 59
EDITS -3 -2 -1 0
* 5 GROUP FUEL REACTION RATES & FUEL AVE FLUX
GROUPS 5 1,1(1) 5
MREG -1=4,34(1) 38
MXS 1(1) 38
EDIT 4 1 3 0
* FUEL AVERAGE 1/V REACTION RATE
GROUPS 1 1,5
MREG -1=4,34(1) 38
MXS 38*33
EDIT 5 1 3 0
* 1/V REACTION RATE AT A COUPLE OF REFLECTOR POINTS
GROUPS 1 1,5
MXS 38*33
LX 5 1,20,21,39,40,59
LY 5 1,22,23,39,40,59
EDITS -6 -2 -1 0
STOP
//
```